A Quantum Mechanical and Molecular Mechanical Method Based on CM1A Charges: Applications to Solvent Effects on Organic Equilibria and Reactions

George A. Kaminski and William L. Jorgensen*

Contribution from the Department of Chemistry, Yale University, New Haven, Connecticut 06520-8107

Received: November 24, 1997

A combined quantum mechanical and molecular mechanical method is presented and tested through Monte Carlo statistical mechanics simulations. The method is general and computationally efficient for obtaining energetic and structural results for organic processes in the liquid phase. The solutes are represented quantum mechanically through AM1 calculations, and the solvent is treated explicitly with classical OPLS potential functions. The interaction between the quantum and classical parts of the systems is computed classically using scaled partial charges for the solute atoms that are derived from the AM1 wave function via the CM1A procedure of Cramer and Truhlar. The new methodology is tested through computation of free energies of hydration of thirteen diverse organic molecules, the medium dependence of the conformational equilibria for 1,2-dichloroethane and furfural, the acceleration of the Claisen rearrangement of allyl vinyl ether in water, and the medium dependence of the tautomeric equilibrium for 2-hydroxypyridine and 2-pyridone.

Introduction

Combined quantum mechanical and molecular mechanical (QM/MM) methods provide a viable approach for modeling the structure, energetics, and reactions of complex systems in condensed phases.[1−20] The chemical system is divided into a region that is treated quantum mechanically and a region that is represented by classical potential energy functions. For example, the quantum mechanical part may consist of a portion of a macromolecule or of one or more smaller solutes. The classical region normally represents the environment such as the rest of the macromolecule and/or hundreds of explicitly simulated solvent molecules. The system can then be simulated via molecular dynamics (MD) or Monte Carlo (MC) methods. Complete quantum mechanical treatment is computationally impractical for such large systems in conjunction with the MD or MC sampling. However, there are numerous advantages of representing the core of the system quantum mechanically including the ability to treat reacting systems with changes in covalency, removal of the need to have molecular mechanics parameters for the core, and the potentially more precise energetic description of the core including, for example, polarization effects and anharmonicity. Pioneered by Warshel, Field, Gao, Merz, and co-workers,[1−7] examples of QM/MM calculations in Monte Carlo and molecular dynamics simulations include studies of organic and bioorganic reactions,[1,2,8,13,16] ion solvation,[17] kinetic isotope effects,[18] enzymatic reactions,[1,11,14,19] ion−molecule association in solution,[9] and conformational equilibria.[10]

The success of the calculations depends on the quantum mechanics, the molecular mechanics, and their coupling. The former issues are determined by the choice of quantum mechanical method and the molecular mechanics force field. For computational efficiency, semiempirical molecular orbital calculations, such as AM1 and PM3, have usually been selected for the quantum mechanics,[21] though ab initio and density functional methods are destined for increased use.[7,11,19] Common choices for force fields are the ones that are often used in condensed-phase simulations, particularly, AMBER, CHARMM, and OPLS.[22−24] For the QM/MM coupling, there are many possibilities. One is to obtain a full potential surface for interaction of the QM part with one molecule of the classical system.[15,25] However, this is computationally tedious and does not incorporate collective polarization effects. The dominant procedure has been to include the Coulombic interactions between the partial charges on the molecular-mechanical atoms and the electrons and nuclei of the quantum part into the quantum mechanical Hamiltonian and to compute the van der Waals interactions between the QM and MM atoms with Lennard-Jones potentials from the MM force field.[1b,2]

In this work, an alternative approach is explored for the QM/MM coupling with AM1 chosen for the quantum mechanics and the OPLS all-atom force field for the molecular mechanics. Specifically, the AM1 wave function is used to obtain partial charges for the quantum mechanical atoms with the recently developed charge model 1 (CM1A) procedure.[26] The CM1A charges for neutral systems are then scaled to reflect the polarization in a condensed-phase environment and used to compute the Coulombic part of the QM/MM coupling, and the OPLS force field provides the Lennard-Jones interactions. The procedure can be referred to as the AOC method for the AM1/OPLS/CM1A combination.

Development of the AOC method proceeded in several stages. The CM1A charges were devised to reproduce gas-phase dipole moments and yield an average error of 0.30 D for a database of 195 molecules.[26] However, polar solvents can increase the polarization of solute molecules as much as 25%.[27] Thus, MC simulations were used to calculate free energies of hydration for thirteen simple molecules, to test the performance of the CM1A charges, and to obtain the best value of a scaling factor to be used in modifying them for the fluid environment. Further testing then began with computation of the well-known solvent effects on the torsional energy profiles of 1,2-dichloroethane and furfural. Subsequently, the acceleration of the Claisen rearrangement of allyl vinyl ether in water and solvent shifts for the tautomeric equilibrium of 2-hydroxypyridine and 2-py-

S1089-5647(98)00314-9 CCC: $15.00
Published on Web 02/18/1998

ridone were examined. These prototypical cases of solvent effects reveal much information about the applicability and limitations of the methodology. Overall, the AOC method performs well and the potential for further developments is evident.

Computaional Approach

The QM/MM Potential. The total effective Hamiltonian for the system is determined from the QM, MM, and QM/MM parts (eq 1). The present solutes are treated quantum

$$\hat{H}_{\text{eff}} = \hat{H}_{\text{QM}} + \hat{H}_{\text{QM/MM}} + \hat{H}_{\text{MM}} \tag{1}$$

mechanically with the AM1 method and the interactions between solvent molecules (TIP4P water,[28] carbon tetrachloride,[29] acetonitrile,[30] dimethyl ether,[31] and dimethyl sulfoxide[32]) were determined by the OPLS potential functions. United-atom methyl groups are used in acetonitrile, dimethyl ether (DME), and dimethyl sulfoxide (DMSO), otherwise all atoms are explicit. These OPLS solvent molecules have no internal degrees of freedom. Thus, the total MM energy is given by the intermolecular interactions between the solvent molecules E_{ab}, which consists of the classical Coulombic and Lennard-Jones contributions between the interaction sites on molecules a and b (eqs 2 and 3). Geometric combining rules are used for σ and ϵ (eqs 4 and 5).

$$E_{\text{MM}} = \sum_{\text{a<b}} E_{\text{ab}} \tag{2}$$

$$E_{\text{ab}} = \sum_{i}^{\text{on a}} \sum_{j}^{\text{on b}} [q_i q_j e^2/r_{ij} + 4\epsilon_{ij}(\sigma_{ij}^{12}/r_{ij}^{12} - \sigma_{ij}^{6}/r_{ij}^{6})] \tag{3}$$

$$\epsilon_{ij} = (\epsilon_{ii}\epsilon_{jj})^{1/2} \tag{4}$$

$$\sigma_{ij} = (\sigma_{ii}\sigma_{jj})^{1/2} \tag{5}$$

Finally, the QM/MM energy of interaction between the quantum-mechanical solutes and the classical solvent molecules was computed in a form similar to eqs 2 and 3:

$$E_{\text{QM/MM}} = \sum_{a} E_{\text{as}} \tag{6}$$

$$E_{\text{as}} = \sum_{i}^{\text{on s}} \sum_{j}^{\text{on a}} [q_i^* q_j e^2/r_{ij} + 4\epsilon_{ij}(\sigma_{ij}^{12}/r_{ij}^{12} - \sigma_{ij}^{6}/r_{ij}^{6})] \tag{7}$$

In this case, however, the double sum is over atoms i of the solute and atoms j of solvent molecule a. Moreover, q_i^* are the partial charges computed with the CM1A procedure from the AM1 wave function and scaled by a factor α, which was kept constant in the present calculations (eq 8). One could optimize different values of α for different solvents, and though calculations have not been carried out yet for charged solutes, $\alpha = 1$ would be the physically sound choice for them. A correction term to the energy for the polarization yielding the scaled charges could also be envisioned; however, consistent with the usual practice with fixed-charge force fields, such a correction was not made in this work.

$$q_i^* = \alpha q_i^{\text{CM1A}} \tag{8}$$

A modified version of the BOSS program, BOSSPAC, was created for the MC simulations with addition of the necessary routines to perform the AM1 and QM/MM energy evaluations and to determine the CM1A charges.[33,34] There are three types of MC moves to generate a new configuration of the system in the isothermal−isobaric (NPT) ensemble. Solute moves were attempted every ca. 50 configurations; this typically entailed random translation and total rotation plus variation of all internal degrees of freedom. Whenever the solute's structure is changed, an AM1 calculation is performed in order to evaluate the new quantum mechanical energy for the solute, the new CM1A charges and the new solute−solvent energies (eqs 6 and 7). If the attempted solute move fails the Metropolis test, then the old solute geometry, AM1 energy, CM1A charges, and solute−solvent energies are reinstated. For solvent moves, a randomly chosen solvent molecule is rigidly translated by random amounts in all three Cartesian directions and rotated a random amount about a randomly chosen Cartesian axis. The energy change is determined from the change in the interactions of the moved solvent molecule with all other solvent molecules and the solute. Last, volume moves consist of scaling the edges of the periodic box randomly and scaling the centers of the solute and solvent molecules out or in by a corresponding amount; in this case, the structure of the solute does not change, so a new AM1 calculation is not needed, though eqs 2, 3, 6, and 7 must be reevaluated owing to the changes in r_{ij}. It is noted that the quantum mechanical energy and wave function for the solute are evaluated in this procedure without explicit inclusion of the field of the solvent molecules; the coupling is provided in an average way through eq 8. A considerable computational advantage results since the QM calculations only have to be performed when the internal structure of the solute changes.

Testing and Applications. The following sequence of computations was undertaken in order to test the applicability of the proposed methodology. Though the CM1A charge model reproduces gas-phase dipole moments well, it was not clear if the charges would perform acceptably in condensed-phase calculations. To begin, an optimal value for α in eq 8 was sought through computing free energies of hydration ΔG_{hyd} for 13 diverse organic molecules. This set had been used previously in a study that tested the utility of solute partial charges that were fit to the electrostatic potential surface (EPS) from ab initio RHF/6-31G* calculations.[27] In that study, the absolute free energies of hydration were computed in TIP4P water with the free energy perturbation (FEP) method. Since the solutes were rigid, all that was required here to obtain ΔG_{hyd} was to perturb the EPS charge distribution for each solute to the one with the scaled CM1A charges (eq 9). The CM1A charges were obtained

$$\Delta G_{\text{hyd}}(\text{CM1A}) = \Delta G_{\text{hyd}}(\text{EPS}) + \Delta G(\text{EPS} \rightarrow \text{CM1A}) \tag{9}$$

from an AM1 calculation on each solute in the standard geometry that was used in the previous study.[27] The Lennard-Jones parameters that were listed in the prior work were also used here.[27] As described below, the optimized value of α turned out to be 1.2; the scaled CM1A charges for the 13 solutes are listed in Table 1 along with the EPS values.

The ΔG for the charge change was computed by the FEP expression in eq 10,[35]

$$\Delta G = -RT(\ln\langle \exp[-(E_1 - E_0)/RT]\rangle_0 \tag{10}$$

where E_0 is the total potential energy for the reference sytem, E_1 is the total potential energy for the perturbed system, and the average is taken for sampling the reference system. Since the charge change is a small perturbation, it was carried out by

TABLE 1: Computed Atomic Charges

molecule	atom	1.2*CM1A	6-31G* EPS
CH_3OH	C	−0.048	0.301
	HC	0.082	−0.010
	O	−0.624	−0.697
	HO	0.426	0.426
CH_3NH_2	C	0.000	0.410
	HC	0.083	−0.046
	N	−1.079	−1.028
	HN	0.415	0.378
CH_3CN	C	−0.147	−0.209
	HC	0.132	0.104
	CN	0.128	0.400
	N	−0.377	−0.503
CH_3OCH_3	C	−0.052	0.095
	HC	0.084	0.038
	O	−0.400	−0.418
CH_3SH	C	−0.236	0.013
	HC	0.121	0.049
	S	−0.277	−0.360
	HS	0.150	0.200
CH_3Cl	C	−0.155	−0.091
	HC	0.115	0.098
	Cl	−0.190	−0.203
C_2H_6	C	−0.255	0.027
	H	0.085	−0.009
CH_3CONH_2	C	−0.295	−0.404
	HC	0.122	0.107
	CO	0.651	0.964
	O	−0.483	−0.680
	N	−1.325	−1.113
	HN	0.543	0.456
CH_3COOH	C	−0.268	−0.311
	HC	0.134	0.102
	CO	0.459	0.859
	O=	−0.476	−0.623
	O-	−0.580	−0.680
	HO	0.463	0.449
$(CH_3)_2CO$	C	−0.322	−0.377
	HC	0.122	0.097
	CO	0.328	0.773
	O	−0.416	−0.601
$AcOCH_3$	C	−0.271	−0.497
	HC	0.131	0.134
	CO	0.465	0.959
	O=	−0.467	−0.633
	O-	−0.386	−0.508
	C	−0.055	−0.130
	HC	0.107	0.049
C_6H_6	C	−0.155	−0.103
	H	0.155	0.103
C_5H_5N	N	−0.343	−0.679
	C1	0.006	0.471
	H1	0.186	0.015
	C2	−0.220	−0.448
	H2	0.170	0.158
	C3	−0.104	0.218
	H3	0.163	0.069

running two simulations between the EPS and CM1A charges at $\lambda = 0.25 \pm 0.25$ and $\lambda = 0.75 \pm 0.25$ where λ is the perturbation coordinate that mixes the two systems. Thus, ΔG(EPS → CM1A) was obtained from the four incremental free energy changes (windows) that came from the two MC simulations for each solute with the double-wide sampling. These calculations were carried out with the BOSS program[33] in the same manner as in the earlier work.[27] Key details were the use of periodic cubes of 260 water molecules and solute−solvent and solvent−solvent interaction cutoffs of 10.0 and 8.5 Å, based approximately on the distance between centers of mass. The Monte Carlo calculations were carried out in the NPT ensemble at 25 C and 1 atm. Volume and solute moves were attempted every 1625 and 60 configurations, respectively. The simulations consisted of at least 1×10^6 configurations of equilibration from an equilibrated water box followed by 2×10^6 configurations of averaging with Metropolis sampling.[34] The ranges for the attempted moves were adjusted to yield an acceptance ratio of ca. 40%.

TABLE 2: OPLS-AA Lennard-Jones Parameters for the Solutes

atom	σ, Å	ϵ, kcal/mol
sp^3 C	3.50	0.066
H on sp^3 C	2.50	0.030
sp^2 C	3.55	0.070
H on sp^2 C	2.42	0.030
C in C═O	3.75	0.105
O in C═O	2.96	0.210
H on O, N	0.00	0.000
Cl	3.40	0.300
alcohol O	3.07	0.170
ether O	2.90	0.140
sp^2 N	3.25	0.170

After establishing α and testing the performance for the free energies of hydration, torsional free energy profiles for the Cl−C−C−Cl dihedral angle of 1,2-dichloroethane (DCE) in

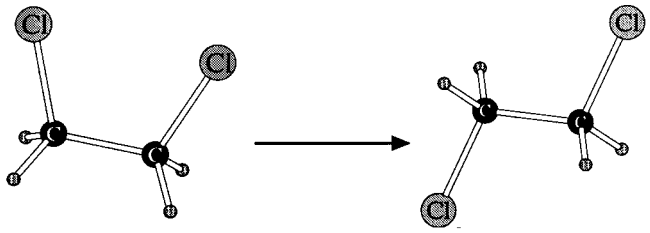

the gas phase and in CCl_4, CH_3CN, and aqueous solutions and for the O−C−C−O dihedral angle of furfural in the gas phase, CCl_4, DMSO, and dimethyl ether (DME) were computed. The

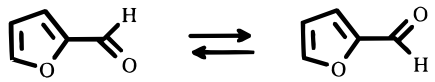

solute molecules were fully flexible except for the dihedral angle that was used as the reaction coordinate. The BOSSPAC program was required since the AM1 calculations had to be performed for each attempted solute move. The torsional profiles were obtained from 10 MC-FEP calculations in each case using a dihedral angle change, $\Delta\varphi$, of 9° with double-wide sampling. The periodic cubes contained 265 solvent molecules and had approximate sizes of $35 \times 35 \times 35$ Å^3 for CCl_4, $20 \times 20 \times 20$ Å^3 for water, $29 \times 29 \times 29$ Å^3 for acetonitrile, $30 \times 30 \times 30$ Å^3 for DME, and $31 \times 31 \times 31$ Å^3 for DMSO. The spherical cutoffs were based on a central atom−central atom distance and were 12.0 Å in all cases except 7.5 Å was used for water−water interactions. Each run consisted of 1×10^6 configurations of equilibration followed by 2×10^6 configurations of averaging in the NPT ensemble at 25 C and 1 atm. Solute and volume moves were attempted every ca. 40 and 1000 configurations, respectively. The Lennard-Jones parameters for these solutes and for the 2-pyridone tautomerization were taken from the OPLS-AA force field[24b] and are listed in Table 2.

The next step was to compute the effect of hydration on the free energy of activation for the Claisen rearrangement of allyl vinyl ether. The change in free energy of hydration was computed for perturbing the reactant to the chair transition structure, as in an earlier study which used RHF/6-31G* structures and EPS charges.[37] Two sets of calculations were

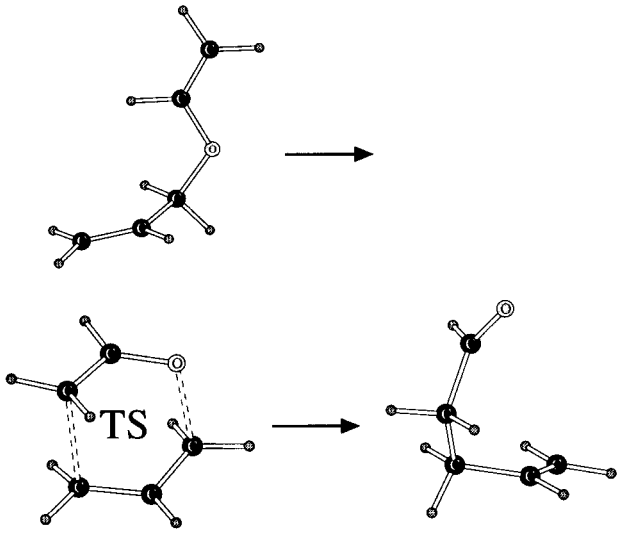

run with different geometries. First, the RHF/6-31G* (gas-phase) structures were used, the CM1A charges were computed, and the reactant's structure was perturbed to the transition structure using MC-FEP calculations. Second, AM1-optimized structures were used for the reactant and transition state, and again the CM1A charges were computed and the perturbation was performed. The solute was rigid, so no QM calculations were necessary during the Monte Carlo simulations, and the standard BOSS program was used. The geometry of the reactant was mutated to the transition structure in a linear fashion, so that for any geometric parameter ξ (bond length, bond angle, or dihedral angle) eq 11 applies where ξ_{reactant} and ξ_{TS} are the

$$\xi(\lambda) = \xi_{\text{reactant}} + \lambda(\xi_{\text{TS}} - \xi_{\text{reactant}}) \qquad (11)$$

values for the reactant and the transition structure and λ is the coupling parameter which changes from 0 to 1 as the system undergoes the mutation. The previously reported Lennard-Jones parameters for the reactant and transition structure were also used here.[37]

Both MC-FEP studies for the Claisen rearrangement were carried out using 11 MC simulations with double-wide sampling and $\Delta\lambda = \pm 0.05$. The system consisted of the solute and 506 TIP4P water molecules in a ca. $25 \times 25 \times 25$ Å^3 periodic cube. Each window covered of 1×10^6 configurations of equilibration and 4×10^6 configurations of averaging in the NPT ensemble at 25 C and 1 atm with 9 Å solute−solvent and solvent−solvent cutoffs. The translations/rotations of the solute and volume moves were attempted every 40 and 1000 configurations, respectively.

Last, the shift in the equilibrium between 2-hydroxypyridine and 2-pyridone was computed in acetonitrile and water at 25 C and 1 atm. In this case, the mutation from reactant

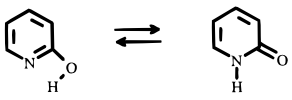

to product was performed in eleven MC simulations with $\Delta\lambda = 0.05$. The AM1 geometries were used along with the scaled CM1A charges, and no internal degrees of freedom were sampled. The system consisted of the solute plus 260 acetonitrile or 505 TIP4P water molecules in a periodic cube. Each window entailed 1×10^6 configurations of equilibration and 4×10^6 configurations of averaging. Solute and volume moves were attempted every 75 and 1000 configurations. Solute−solvent and solvent−solvent cutoff distances were 9.5 Å in water and 12.0 Å in acetonitrile.

TABLE 3: Calculated and Experimental Free Energies of Hydration[a]

molecule	ΔG_{hyd}, EPS[b]	ΔG_{hyd}, CM1A	ΔG_{hyd}, 1.2*CM1A	ΔG_{hyd}, exptl[c]
CH_3OH	-4.6 ± 0.4	-1.4 ± 0.4	-4.4 ± 0.4	-5.1
CH_3NH_2	-4.3 ± 0.5	-3.4 ± 0.5	-6.5 ± 0.5	-4.6
CH_3CN	-4.7 ± 0.5	-2.8 ± 0.5	-5.0 ± 0.5	-3.9
CH_3OCH_3	-1.4 ± 0.5	-0.9 ± 0.5	-2.6 ± 0.5	-1.9
CH_3SH	0.0 ± 0.5	1.4 ± 0.5	0.7 ± 0.5	-1.2
CH_3Cl	0.1 ± 0.5	0.8 ± 0.5	0.1 ± 0.5	-0.5
C_2H_6	2.7 ± 0.4	2.6 ± 0.4	2.5 ± 0.5	1.8
CH_3CONH_2	-13.4 ± 0.4	-6.4 ± 0.6	-11.9 ± 0.5	-9.7
CH_3COOH	-8.5 ± 0.4	-3.8 ± 0.4	-7.7 ± 0.4	-6.7
$(CH_3)_2CO$	-5.4 ± 0.5	-1.7 ± 0.5	-3.6 ± 0.5	-3.8
$AcOCH_3$	-5.3 ± 0.5	-1.8 ± 0.5	-4.6 ± 0.5	-3.3
C_6H_6	-0.4 ± 0.4	-1.7 ± 0.4	-2.9 ± 0.4	-0.8
C_5H_5N	-4.9 ± 0.4	-4.1 ± 0.4	-5.1 ± 0.4	-4.7
ave. error	1.2	1.8	1.1	−

[a] Energies in kcal/mol. [b] Reference 27. [c] Reference 38.

The calculations described above were performed over a two-year period, which gave rise to minor variations in details such as the cutoff distances and frequencies of solute moves. However, the protocols are all reasonable and the lengths of the runs and numbers of FEP windows are typical for provision of high precision.

Results and Discussion

Free Energies of Hydration. Computed and experimental free energies of hydration for the 13 solutes are compared in Table 3. The results include the previously reported data using the 6-31G* EPS charges[27,39] and the findings with the unscaled CM1A charges and with $\alpha = 1.2$. The statistical uncertainties ($\pm 1\sigma$) were obtained by the batch means procedure[36] and are dominated by the uncertainty in the EPS results. The average error of 1.8 kcal/mol with the unscaled CM1A charges is reduced with $\alpha = 1.2$ to 1.1 kcal/mol, which is slightly better than the 1.2 kcal/mol error with the 6-31G* EPS charges. Other values of α were tried with little effect on the fit for $\alpha = 1.20 \pm 0.05$; larger values of α lead to unacceptable errors for benzene and acetamide. The choice of $\alpha = 1.2$ is consistent with the general observation that the charge distributions for force fields intended for use in condensed-phase simulations need to yield dipole moments enhanced 15−20% over gas-phase values.[24,27]

Taking a closer look at the results, there are five solutes that yield errors under 1 kcal/mol with both the scaled CM1A and EPS charges: methanol, dimethyl ether, methyl chloride, ethane, and pyridine. Comparison of the charges in Table 1 indicates that the similar results do not always arise from similar charge distributions. For dimethyl ether and methyl chloride, the charge distributions are similar, but for the other molecules there are significant differences, particularly for methyl groups. Methyl carbons attached to heteroatoms are often much more positive with the EPS charges (e.g., 0.3−0.4 *e* more positive for methanol and methylamine). This weakens hydrogen bonds to the adjacent heteroatom. Thus, for hydrogen-bond donation to methanol, the more negative oxygen with the EPS charges is compensated by the more positive carbon. For pyridine, the two charge distributions in Table 1 are very different with the nitrogen more negative by 0.34 *e* from the EPS data, which is

compensated to some extent by the more positive adjacent carbons. It may be noted that the dipole moment for pyridine with the EPS charges, 2.37 D, is greater than the gas-phase experimental value of 2.19 D,[26] as usual, while the scaled CM1A charges yield a dipole moment of only 1.79 D. This is the only 1 of the 13 molecules for which the dipole moment from the scaled CM1A charges is less than the gas-phase experimental value. The CM1A dipole moments for heterocycles show greater than average errors,[26] so some caution is advised for applications with this class of molecules.

The largest errors for the computed free energies of hydration are for acetamide, methylamine, and benzene with the scaled CM1A charges. The latter two molecules are treated well with the EPS charges. The dipole moment of methylamine from the scaled CM1A charges, 2.08 D, is much greater than the experimental and EPS values of 1.31 and 1.79 D. The larger charges on the nitrogen and amino hydrogens along with the small charge on carbon from the scaled CM1A description all lead to stronger hydrogen bonding and an overly exoergic ΔG_{hyd}. Benzene is also too hydrophilic with the scaled CM1A charges, now by 2.1 kcal/mol. Though the ΔG_{hyd} for ethane shows little sensitivity to the charge distribution,[40] the more negative carbons for benzene with the scaled CM1A charges (−0.155 e) than from the EPS (−0.103 e) or OPLS-AA (−0.115 e) assignments lead to overly favorable π-hydrogen bonds with water molecules. Optimizations with a TIP4P water molecule yield complexation energies of −5.04, −3.44, and −3.79 kcal/mol with the three charge sets, respectively, for the structure below. The best available ab initio and experimental results are −3 ± 1 kcal/mol for this quantity.[41]

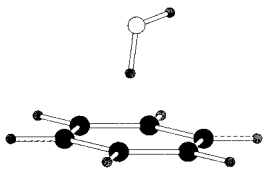

Carbonyl compounds are particularly problematic with the EPS charges. For acetone, the dipole moments from the scaled CM1A and EPS charges are both 3.4 D, which is a reasonable overestimate of the experimental value of 2.88 D. However, the scaled CM1A result for ΔG_{hyd} is too hydrophobic by 0.2 ± 0.5 kcal/mol, while the EPS result is too hydrophilic by 1.6 ± 0.5 kcal/mol. This reflects too much polarization for the C═O bond with the EPS charges (Table 1). The lessened polarization with the scaled CM1A charges for the other carbonyl compounds also leads to significant improvement for ΔG_{hyd} over the EPS results (Table 3).

Overall, similar accuracy for free energies of hydration is obtained with the scaled CM1A charges or 6-31G* EPS charges. Of course, it is much faster to do a single-point AM1/CM1A calculation with BOSSPAC than a single-point RHF/6-31G* calculation with Gaussian94. For acetamide, the AM1/CM1A calculations are about 5000 times faster; the timings on an SGI R5000SC are 0.046 and 221 s, respectively, and the difference rapidly gets larger with larger molecules. Furthermore, the average error from Gao's AM1-based QM/MM calculations for free energies of hydration relative to ethane for 10 neutral solutes is 1.4 kcal/mol.[4] Thus, there is also no practical advantage to the more complex QM/MM procedure.[4]

Torsional Free-Energy Profiles for 1,2-Dichloroethane and Furfural. The conformational equilibrium between the gauche and trans forms of 1,2-dichloroethane is well-known to depend strongly on the polarity of the medium.[42−45] The population

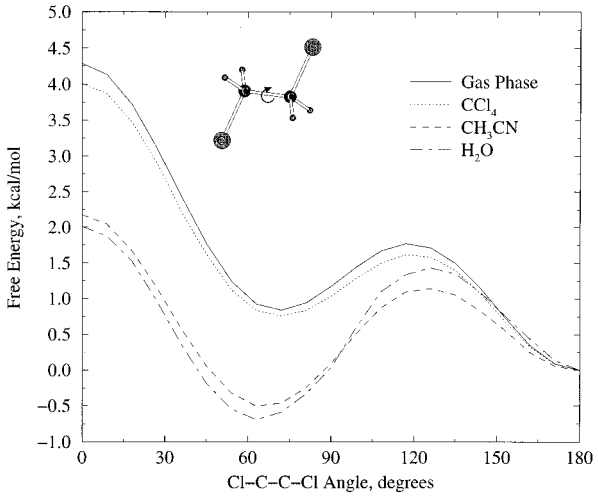

Figure 1. Free energy profiles for rotation about the C−C bond in 1,2-dichloroethane from Monte Carlo simulations with the AOC method.

TABLE 4: Gauche−Trans Free Energy Differences for 1,2-Dichloroethane[a]

medium	OPLS-AA[b]	AOC[c]	exptl[d]
gas phase	1.17	0.86	1.20
CCl_4		0.76	0.50
CH_3CN	−0.33	−0.33	−0.22
H_2O		−0.62	

[a] Energy differences in kcal/mol. [b] Reference 46. [c] This work. [d] References 43−44.

of the gauche form with a dipole moment of ca. 3.5 D increases in polar solvents at the expense of the trans form with a dipole moment of zero. Though the trans form is observed to be more stable in the gas phase than the gauche rotamer by 1.20 kcal/mol, the difference is decreased to 0.70 kcal in cyclohexane, 0.11 kcal/mol in tetrahydrofuran, and the sign changes to yield −0.14 kcal/mol in acetone and −0.22 kcal/mol in acetonitrile.[42−45]

The computed free energy profiles for variation of the Cl−C−C−Cl dihedral angle are shown in Figure 1 and the gauche−trans free energy differences are summarized in Table 4. The latter were obtained from integration over the profiles in Figure 1. The solvent-induced shift with the present AOC calculations is in the expected direction. The gas-phase difference of 0.86 kcal/mol is a little lower than the experimental 1.20 kcal/mol; however, the computed shift of 1.19 kcal/mol in going to acetonitrile is in good accord with the observed result of 1.42 kcal/mol. This system has been the target of numerous other studies; for example, a shift of 1.55 kcal/mol was obtained from 6-31+G* SCRF calculations with the simple dipolar Onsager reaction field,[45] and 1.12 kcal/mol arose from more sophisticated B3LYP/6-311+G** SCRF calculations with a polarizable continuum model.[44] Furthermore, all calculations concur that there is a small shift toward cis in the equilibrium dihedral angle for the gauche conformer in polar solvents. For the AOC results, the change is from 72° in the gas phase to 65° in the most polar solvents.

Carbon tetrachloride was included as a solvent, rather than chloroform or methylene chloride, to illustrate that the AOC procedure would not predict the equilibrium shift in a nonpolar solvent (Table 4). This is true for any model that does not provide for the induction of dipoles in nonpolar solvent molecules by a polar solute, as previously presented.[46] No force-field calculations with fixed solute charges and nonpolarizable solvent molecules can reproduce the observed effect.

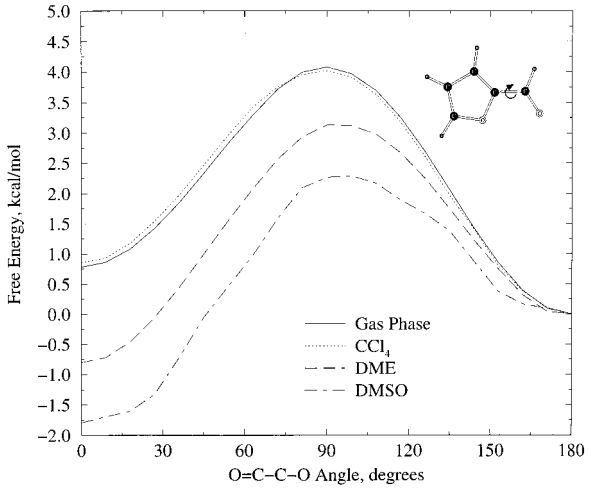

Figure 2. Free energy profiles for rotation about the exocyclic C−C bond in furfural from Monte Carlo simulations with the AOC method.

TABLE 5: Syn−Anti Free Energy Differences for Furfural[a]

medium	SCRF[b]	AOC[c]	exptl[d]
gas phase	0.90	0.68	1−2
CCl_4	0.38	0.78	0.2
DME	−0.14	−0.77	−0.21
DMSO	−0.38	−1.72	−0.84

[a] Energy differences in kcal/mol. [b] Reference 45. [c] This work. [d] Reference 47.

QM/MM procedures that include the electric field of the solvent molecules in the Hamiltonian, but that do not let the solvent molecules be polarizable, will also underestimate the response in nonpolar solvents. SCRF calculations with even the simple Onsager reaction field do pick up this effect; their problems are more with the specific interactions in hydrogen-bonding solvents.[44,45] This suggests a possibility for future QM/MM development: semiempirical MO−SCRF calculations for the solutes, MM for the solvent, and use of the SCRF-based charges for the QM/MM electrostatic interactions.

The corresponding results for rotation about the O−C−C−O bond in furfural are provided in Figure 2 and Table 5. In this case, the more polar syn conformer is preferentially stabilized in polar solvents. With the scaled CM1A charges, the computed dipole moments for the syn and anti conformers are 4.37 and 3.36 D, which are close to the 6-31G* optimized values of 4.35 and 3.50 D.[45] Experimentally,[47] the gas-phase syn−anti energy difference is 1.0−2.0 kcal/mol, solvation in carbon tetrachloride decreases it to 0.20 kcal/mol, and the syn conformer becomes preferred by 0.21 kcal/mol in dimethyl ether and by 0.84 kcal/mol in DMSO. Again the computed shifts in the equilibrium in polar solvents with the AOC method agree well with the experimental data. Using the experimental average of 1.5 kcal/mol for the gas-phase energy difference, the observed shifts in going to DME and DMSO of 1.7 and 2.3 kcal/mol are within the noise level of the AOC predictions of 1.5 and 2.4 kcal/mol (Table 5). The results from 6-31G* SCRF calculations with the dipolar Onsager model are also listed and predict smaller shifts of 1.0 and 1.3 kcal/mol, respectively.[45] As for dichloroethane, the AOC results in the nonpolar solvent, carbon tetrachloride, miss the solvent effect as would any model that lacks solvent polarization.[46]

Claisen Rearrangement of Allyl Vinyl Ether. Among [3,3] sigmatropic reactions, the Claisen rearrangement attracts special attention because of its synthetic and mechanistic importance in organic and biological chemistry.[48] A particularly interesting point is the ca. 1000-fold rate acceleration for reaction of the parent allyl vinyl ether in water compared to the gas phase,[37] as well as ca. 200-fold acceleration for a 4-substituted derivative in going from cyclohexane solution to water.[48a] The origin of the rate acceleration can be traced predominantly to enhanced polarization of the transition structure; in water, this leads to progressing from the reactant with one weak hydrogen bond on the enolic oxygen to the transition structure with two strong hydrogen bonds on the oxygen.[37] This picture, which emerged from Monte Carlo simulations[37] using ab initio geometries and 6-31G* EPS charges,[49] also appears to be central to the mechanism of enzymatic catalysis of the Claisen rearrangement of chorismate.[48b,50] The parent Claisen rearrangement in water has been studied computationally by several other methods including AM1-SM2,[51] AM1-based QM/MM,[52,53] and ab initio SCRF calculations.[37b,54]

TABLE 6: Changes in Free Energy of Activation for the Claisen Rearrangement of Allyl Vinyl Ether upon Transfer from the Gas Phase to Aqueous Solution

method	$\Delta\Delta G^{\ddagger}$
experiment[b]	ca. −4.0
MC-FEP, 6-31G* geometries[b]	-3.85 ± 0.16
QM/MM, 6-31G* geometries[c]	-3.5 ± 0.1
AM1-SM2, 6-31G* geometries[d]	−1.66
AM1-SM2, AM1 geometries[d]	−0.75
AOC, 6-31G* geometries[e]	-3.60 ± 0.16
AOC, AM1 geometries[e]	-1.66 ± 0.16

[a] Energy in kcal/mol. [b] Reference 37. [c] Reference 52. [d] References 37, 51. [e] This work.

As noted above, the change in free energy of hydration was computed with the AOC method by perturbing the reactant to the transtion structure. Two sets of geometries were used (i.e., the ones from the RHF/6-31G* optimizations[49] and those from AM1 calculations). In both cases, the scaled CM1A charges with $\alpha = 1.2$ were employed. The results are given in Table 6 along with experimental and prior computed data. As found previously, there is a significant difference in the outcome with the 6-31G* and AM1 geometries.[37,51,53] The AOC result of −3.6 kcal/mol with the 6-31G* geometries is close to the MC results with the 6-31G* geometries and EPS charges, −3.9 kcal/mol, and the experimental value of ca. −4 kcal/mol. The only significant difference between these two calculations is the use of the scaled CM1A or 6-31G* EPS charges. The two sets of charges are seen to be similar in Figure 3a,b; in particular, the net charges on the allylic and enolic fragments are ±0.31 and ±0.27 *e* and the oxygen charge is −0.45 and −0.49 *e* with the scaled CM1A and EPS charges, respectively. However, with the AM1 geometries and corresponding scaled CM1A charges (Figure 3c), the predicted solvent effect is too weak, −1.7 kcal/mol. While the reactant geometry and scaled CM1A dipole moments do not depend on the model significantly (1.96 and 1.95 D for the 6-31G* and AM1 geometries), the AM1 transition structure has too little C−O bond breaking (1.580 Å) and too small a dipole moment (2.16 D) compared to those for the 6-31G* structure (1.918 Å and 3.08 D). The computed charges on the allylic and enolic fragments are reduced in magnitude to ±0.18 *e* and the oxygen is less negative, −0.37 *e*.

Overall, the computed solvent effect is in excellent agreement with the experimental data as long as the 6-31G* geometries are used with the scaled CM1A charges, the EPS charges, or Gao's AM1-based QM/MM calculations. These models have all used explicit TIP3P or TIP4P water molecules for the solvent. SCRF calculations with continuum solvent models including AM1/SM2 and ab initio-based procedures all yield too small solvent effects for the Claisen rearrangement.[37,51,53,54] The

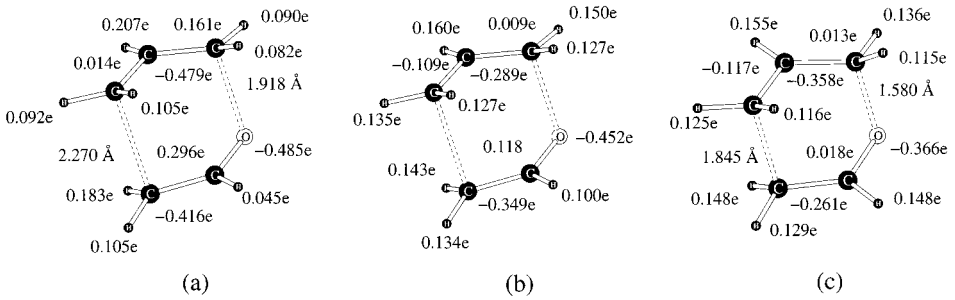

Figure 3. Transition structures and partial charges for the Claisen rearrangement of allyl vinyl ether: (a) RHF/6-31G* structure and EPS charges, (b) RHF/6-31G* structure and scaled ($\alpha = 1.2$) CM1A charges, and (c) AM1 structure and scaled ($\alpha = 1.2$) CM1A charges.

TABLE 7: Difference in Free Energy of Solvation for the Tautomeric Equilibrium of 2-Hydroxypyridine → 2-Pyridone[a]

solvent	QM/MM[b]	AM1-SM2[c]	AOC[d]	exptl[e]
CH_3CN			-2.35 ± 0.09	-3.7 ± 0.7
water	-5.7 ± 0.2	-2.6	-2.23 ± 0.22	-4.4 ± 0.8

[a] Energy in kcal/mol. [b] Reference 55. [c] Reference 56a. [d] This work. [e] See text.

integral change from 1 to 2 in number of solute-water hydrogen bonds on passing to the transition structure, which is found in the MC simulations,[37] is undoubtedly problematic for continuum theories.

Tautomeric Equilibrium of 2-Hydroxypyridine and 2-Pyridone. Another important process that is prone to solvent effects is the tautomeric equilibrium of heterocyclic compounds.[42,55−63] The case of 2-hydroxypyridine and 2-pyridone is well-known to favor the hydroxy form in the gas phase and to shift increasingly to the lactam tautomer in polar media. Related behavior is common with other heterocycles including nucleotide bases.[42,58,59]

Gas-phase AM1 calculations give an energy difference of 0.4 kcal/mol for the 2-hydroxypyridine → 2-pyridone conversion, which agrees well with the experimental ΔG of 0.3 kcal/mol.[42] Computed changes in free energy of solvation are compared with experimental results in Table 7. Only the syn form of 2-hydroxypyridine with $\varphi(\mathrm{N-C-O-H}) = 0°$ was considered in the AOC calculations since the anti conformer has previously been shown to not be competitive.[57,58] A few comments need to be made concerning the experimental data. The equilibrium constants K_T in ref 42 are typically used to provide the free energy changes. The K_T of 0.4 ± 0.25 in the gas phase[60] at 130 °C and 148 ($\log K_T = 2.17 \pm 0.3$)[61] in acetonitrile at 25 °C are from direct UV measurements. However, the listed K_T in water of 910 without error bars is not from a direct measurement, but comes from the difference in pK_a values for N- and O-methylated 2-hydroxypyridine.[62] The pK_as for the O-methyl compound and 2-hydroxypyridine itself have also been used and give $K_T = 340$.[63] Thus, there is considerable uncertainty in the experimental results, as reflected in the average values for $\Delta\Delta G$ that are reported in Table 7.

The AOC prediction in acetonitrile underestimates the observed shift by about 1 kcal/mol, while the predicted solvent effect in water, -2.2 ± 0.2 kcal/mol, appears to be too small in magnitude by about 2 kcal/mol. Other computed values in water cover a significant range including the −5.7 kcal/mol from the QM/MM calculations of Gao and Shao,[57] and −2.6 and −4.3 kcal/mol from AM1-SM2 and AM1-SM3 calculations.[56a] A shift of −3.0 kcal/mol was obtained from SCRF calculations with the Onsager reaction field at $\epsilon = 36$ (acetonitrile) and would change little for $\epsilon = 80$ (water).[55]

To gain some insights into the AOC underestimate of the

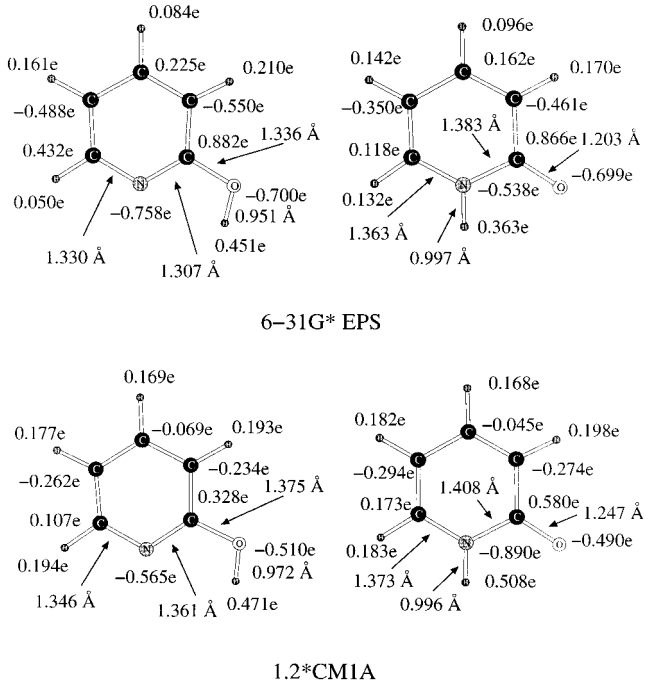

Figure 4. Partial atomic charges and some geometrical parameters for 2-hydroxypyridine and 2-pyridone from the RHF/6-31G* calculations and EPS charges (top) and from the AM1 calculations and scaled CM1A charges (bottom).

hydration effect, several additional calculations were carried out. First, the effect of switching to 6-31G* EPS charges and geometries was evaluated by MC-FEP calculations. The computed free energy changes in water for converting from the AM1 geometry and scaled CM1A charges to the 6-31G* alternatives are 3.45 ± 0.08 kcal/mol for 2-hydroxypyridine and -0.79 ± 0.08 kcal/mol for 2-pyridone, which shifts the equibrium by 4.2 kcal/mol. This means that the predicted $\Delta\Delta G$ in water is −6.4 kcal/mol (−2.2−4.2) with the 6-31G* EPS charges and geometries, which now overshoots the observed effect by ca. 2 kcal/mol (Table 7). It could be expected that the predicted shifts with the AOC calculations would be larger if the geometries of the solutes changed in the solutions. However, the geometrical changes from the SCRF calculations are small; the largest bond length difference between the gas phase ($\epsilon = 1$) and $\epsilon = 36$ is 0.008 Å.[55] Such differences are much smaller than the changes caused by using different QM procedures (e.g., 0.03 Å for some bond lengths between RHF/6-31G* and MP2/6-31G** optimizations).[55]

One might expect that the 4.2 kcal/mol shift should be reflected in the computed dipole moments. However, the scaled CM1A charges give dipole moments of 1.71 and 4.80 D for the hydroxy and lactam tautomers, and the 6-31G* EPS values are not very different at 1.49 and 4.99 D. Too much significance

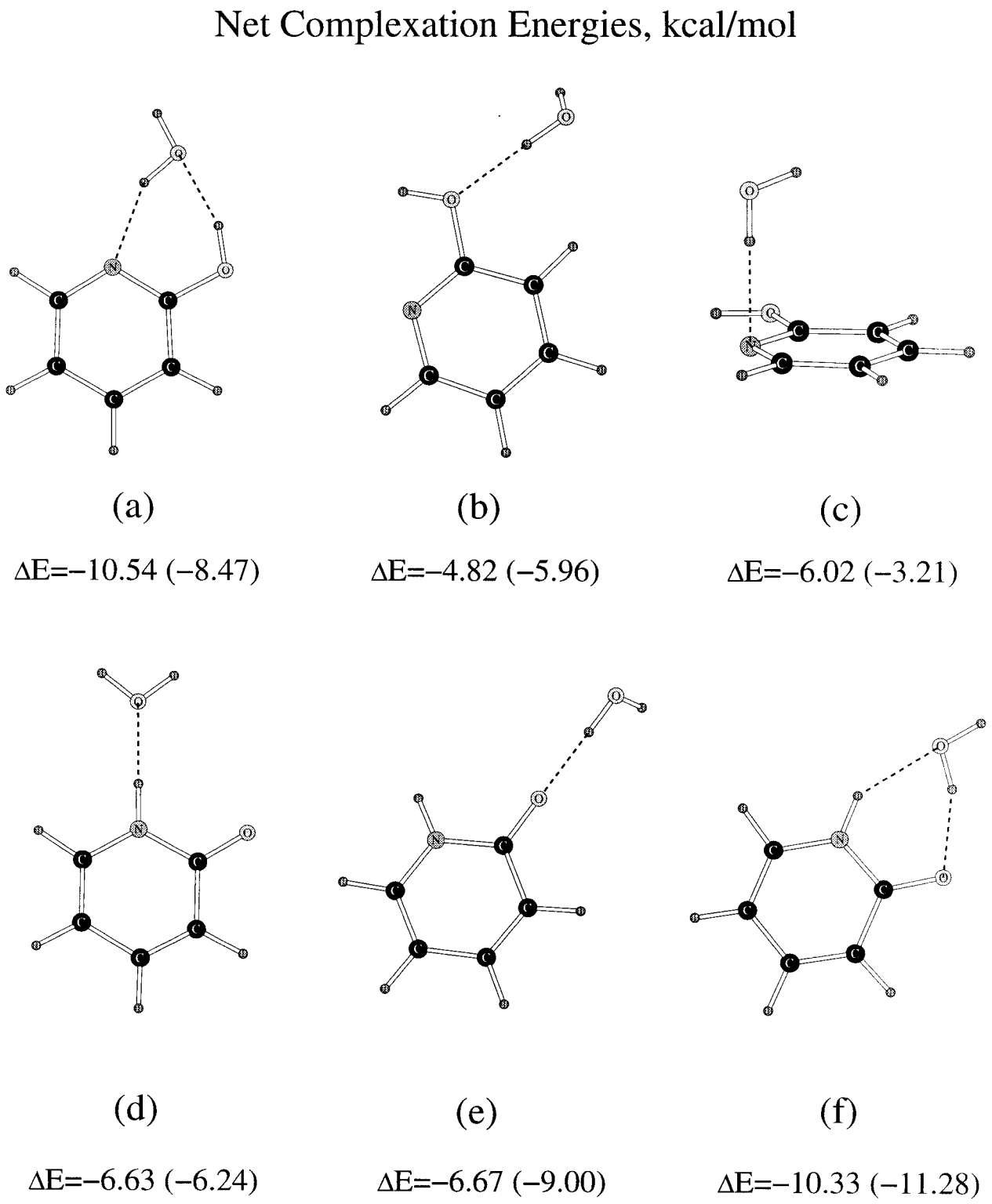

Figure 5. Optimized complexes of 2-hydroxypyridine and 2-pyridone with a TIP4P water molecule. The interaction energies from calculations with the scaled CM1A charges and AM1 geometries are shown with the corresponding values using RHF/6-31G* geometries and EPS charges in parentheses. Only intermolecular dgerees of freedom were optimized with the following restrictions: (a) the complex is planar, (b) the water O−H bond is in the ring plane, (c) the water O−H bond is perpendicular to the ring and the N, H, and O atoms are collinear, (d) N, H, and O are collinear, (e) C═O···H−O are collinear, and (f) the complex is planar.

can be placed on dipole moment changes as a monitor of electrostatic interactions.[53] Details of the charge distributions or higher multipole moments are clearly important. The scaled CM1A and 6-31G* EPS charges are shown in Figure 4 and indeed show substantial differences despite the similarity in dipole moments. For 2-hydroxypyridine, the nitrogen is more negative with the EPS charges by 0.2 e; however, the adjacent carbons are more positive by 0.3−0.5 e. For 2-pyridone, the EPS oxygen is more negative by 0.2 e, while the carbonyl carbon and nitrogen are more positive by 0.3 e.

These charge shifts are bound to lead to significant differences in hydrogen-bond strengths with water. Display of configurations from the Monte Carlo simulations revealed the same patterns of hydrogen bonding with the two charge sets.

Specifically, for 2-hydroxypyridine, the hydroxyl group participates in two hydrogen bonds, one as the donor and one as the acceptor, and the nitrogen is the acceptor for two hydrogen bonds, typically out-of-plane. For 2-pyridone, the oxygen accepts two hydrogen bonds, mostly in-plane, and the amino hydrogen is the donor in another. The strengths of corresponding, representative interactions were explored through constrained geometry optimizations for the complexes in Figure 5 with a TIP4P water molecule. The monomers were kept fixed in the calculations and only intermolecular degrees of freedom were optimized. Consistent with the 3.45 kcal/mol poorer ΔG_{hyd} of 2-hydroxypyridine with the EPS charges, the complexes in Figure 5a,c are 2−3 kcal/mol more strongly hydrogen-bonded with the scaled CM1A charges. For the latter case with the hydrogen bond perpendicular to the ring plane, the more favorable interaction with the CM1A charge distribution owes much to the diminished electrostatic repulsion between the hydrogens of water and the carbons adjacent to the nitrogen. The two sets of results are more similar for 2-pyridone, though stronger hydrogen bonding to the more negative amide oxygen is apparent with the 6-31G* EPS charges.

Overall, the calculations in this section demonstrated that the AOC approach provides results competitive with other methods for estimating solvent effects on a tautomerization. The sensitivity of the findings to the details of the utilized charge distributions was also highlighted.

Conclusions

An efficient method for combined quantum and molecular mechanical calculations has been presented and tested on predictions of solvent effects for fundamental organic equilibria and reactions. In the AOC method the solutes are represented quantum mechanically by AM1 calculations, the solvent molecules are represented with the OPLS force field, and their coupling utilizes scaled CM1A charges for the solutes and OPLS Lennard-Jones parameters. A key advantage of the incorporation of quantum mechanical calculations in condensed-phase simulations is the elimination of the need for a complete, accurate force-field for the solutes, which is often unavailable for polyfunctional systems. The AM1/CM1A calculations were demonstrated to provide charge distributions that perform as well as 6-31G* EPS charges, which have been a standard choice. However, in contrast to the 6-31G* calculations, the speed of the CM1A/AM1 calculations is sufficient for their routine application in condensed-phase simulations of large molecular systems. The main difference with typical QM/MM techniques is that the electric field of the solvent molecules has only been incorporated in an avergage sense through the scaling of the CM1A charges. This simplification makes the quantum mechanical calculations only required when the solutes are moved in Monte Carlo simulations, which introduces minimal additional computational effort. The proposed AOC method was tested on predictions of free energies of hydration for 13 prototypical molecules, the shifts in conformational equilibria for 1,2-dichloroethane and furfural in several solvents, the rate enhancement for the Claisen rearrangement of allyl vinyl ether in water, and the tautomerization of 2-hydroxypyridine and 2-pyridone in acetonitrile and water. In all cases, reasonable results were obtained that are at least competitive with alternative QM/MM methods. The sensitivity of the results to the details of the solutes' charge distributions was emphasized. In addition to identifying potential areas for improvement including the underlying semiempirical molecular orbital method, even more optimal charge distributions, and treatment of the polarization of nonpolar solvents, the present results have also provided a baseline for justification of more complex QM/MM methods.

Acknowledgment. Gratitude is expressed to the National Science Foundation for support of this work and to Professors C. J. Cramer and D. G. Truhlar for providing the AMSOL program.[34]

References and Notes

(1) For reviews, see: (a) Åqvist, J.; Warshel, A. *Chem. Rev.* **1993**, *93*, 2523. (b) Gao, J. *Acc. Chem. Res.* **1996**, *29*, 298.
(2) Field, M. J.; Bash, P. A.; Karplus, M. *J. Comput. Chem.* **1990**, *11*, 700.
(3) Field, M. J. *J. Chem. Phys.* **1992**, *96*, 4583.
(4) Gao, J.; Xia, X. *Science* **1992**, *258*, 631.
(5) Gao, J. *J. Am. Chem. Soc.* **1993**, *115*, 2930.
(6) Wesolowski, T. A.; Warshel, A. *J. Phys. Chem.* **1993**, *97*, 8050.
(7) Stanton, R. V.; Hartsough, D. S.; Merz, K. M., Jr. *J. Phys. Chem.* **1993**, *97*, 11868.
(8) Thompson, M. A.; Schenter, G. K. *J. Phys. Chem.* **1995**, *99*, 6374.
(9) Thompson, M. A. *J. Am. Chem. Soc.* **1995**, *117*, 11341.
(10) Thompson, M. A. *J. Phys. Chem.* **1995**, *99*, 4794.
(11) Hartsough, D. S.; Merz, K. M., Jr. *J. Phys. Chem.* **1995**, *99*, 11266.
(12) Gao, J.; Habibollazadeh, D.; Shao, L. *J. Phys. Chem.* **1995**, *99*, 16460.
(13) Gao, J. *J. Am. Chem. Soc.* **1995**, *117*, 8600.
(14) Lyne, P. D.; Mulholland, A. J.; Richards, W. G. *J. Am. Chem. Soc.* **1995**, *117*, 11345.
(15) Wang, J.; Boyd, R. J.; Laaksonen, A. *J. Chem. Phys.* **1996**, *104*, 7261.
(16) Furlani, T. R.; Gao, J. *J. Org. Chem.* **1996**, *61*, 5492.
(17) Kerdcharoen, T.; Liedl, K. R.; Rode, B. M. *Chem. Phys.* **1996**, *211*, 313.
(18) Barnes, J. A.; Williams, I. H. *J. Chem. Soc., Chem. Commun.* **1996**, 193.
(19) Freindorf, M.; Gao, J. *J. Comput. Chem.* **1996**, *17*, 386.
(20) Cunningham, M. A.; Ho, L. L.; Nguyen, D. T.; Gillilan, R. E.; Bash, P. A. *Biochemistry* **1997**, *36*, 4800.
(21) (a) Dewar, M. J. S.; Zoebisch, E. G.; Healy, E. F.; Stewart, J. J. P. *J. Am. Chem. Soc.* **1985**, *107*, 3902. (b) Stewart, J. J. P. *J. Comput. Chem.* **1989**, *10*, 209, 221.
(22) Weiner, S. J.; Kollman, P. A.; Nguyen, D. T.; Case, D. A. *J. Comput. Chem.* **1986**, *7*, 230. Cornell, W. D.; Cieplak, P.; Bayly, C. I.; Gould, I. R.; Merz, K. M., Jr.; Ferguson, D. M.; Spellmeyer, D. C.; Fox, T.; Caldwell, J. W.; Kollman, P. A. *J. Am. Chem. Soc.* **1995**, *117*, 5179.
(23) Brooks, B. R.; Bruccoleri, R. E.; Olafson, B. D.; States, D. J.; Swaminathan, S.; Karplus, M. *J. Comput. Chem.* **1983**, *4*, 187.
(24) (a) Jorgensen, W. L.; Tirado-Rives, J. *J. Am. Chem. Soc.* **1988**, *110*, 1657. (b) Jorgensen, W. L.; Maxwell, D. S.; Tirado-Rives, J. *J. Am. Chem. Soc.* **1996**, *118*, 11225.
(25) Chandrasekhar, J.; Smith, S. F.; Jorgensen, W. L. *J. Am. Chem. Soc.* **1985**, *107*, 154.
(26) Storer, J. W.; Giesen, D. J.; Cramer, C. J.; Truhlar, D. G. *J. Comput.-Aided Mol. Des.* **1995**, *9*, 87.
(27) Carlson, H. A.; Nguyen, T. B.; Orozco, M.; Jorgensen, W. L. *J. Comput. Chem.* **1993**, *14*, 1240.
(28) Jorgensen, W. L.; Chandrasekhar, J.; Madura, J. D.; Impey, R. W.; Klein, M. L. *J. Chem. Phys.* **1983**, *79*, 926.
(29) Duffy, E. M.; Severance, D. L.; Jorgensen, W. L. *J. Am. Chem. Soc.* **1992**, *114*, 7535.
(30) Jorgensen, W. L.; Briggs, J. M. *Mol. Phys.* **1988**, *63*, 547.
(31) Briggs, J. M.; Matsui, T.; Jorgensen, W. L. *J. Comput. Chem.* **1990**, *11*, 958.
(32) The charge in e, σ in Å, and ϵ in kcal/mol are 0.160, 3.81, and 0.160 for CH_3, 0.139, 3.56, and 0.395 for S, and −0.459, 2.93, and 0.280 for O. The geometrical parameters are r(C−S) = 1.80 Å, r(S−O) = 1.53 Å, ∠C−S−C = 97.4°, and ∠C−S−O = 106.75°. The model was fit to reproduce observed properties of DMSO at 25 °C.
(33) Jorgensen, W. L. *BOSS Version 3.6*; Yale University: New Haven, CT, 1995.
(34) The routines required for the AM1 and CM1A calculations were extracted from the AMSOL program: Cramer, C. J.; Hawkins, G. D.; Lynch, G. C.; Giesen, D. J.; Truhlar, D. G.; Liotard, D. A. *AMSOL Version 4.6c*; University of Minnesota: Minneapolis, MN, 1994.
(35) Zwanzig, R. W. *J. Chem. Phys.* **1954**, *22*, 1420.
(36) For a review, see: Allen, M. P.; Tildesley, D. J. *Computer Simulations of Liquids*; Clarendon Press: Oxford, U.K., 1987.
(37) (a) Severance, D. L.; Jorgensen, W. L. *J. Am. Chem. Soc.* **1992**, *114*, 10966. (b) Severance, D. L.; Jorgensen, W. L. In *Structure and Reactivity in Aqueous Solution*; Cramer, C. J., Truhlar, D. G., Eds.; ACS

Symposium Series 568; American Chemical Society: Washington, DC, 1994; pp 243−259.

(38) (a) Hine, J.; Mookerjee, P. K. *J. Org. Chem.* **1975**, *40*, 292. (b) Ben-Naim, A.; Marcus, Y. *J. Chem. Phys.* **1984**, *81*, 2016. (c) Wolfenden, R.; Liang, Y.-L.; Matthews, M.; Williams, R. *J. Am. Chem. Soc.* **1987**, *109*, 463.

(39) Several of the FEP results from ref 27 were recomputed here with greater precision. The only inconsistencies found were for the acetic acid to acetone and methanol to ethane mutations; the corrected values for ΔG_{hyd} of acetone and ethane are given in Table 3.

(40) Kaminski, G.; Duffy, E. M.; Matsui, T.; Jorgensen, W. L. *J. Phys. Chem.* **1994**, *98*, 13077.

(41) Jorgensen, W. L.; Severance, D. S. *J. Am. Chem. Soc.* **1990**, *112*, 4768. Gotch, A. J.; Zwier, T. S. *J. Chem. Phys.* **1992**, *96*, 3388.

(42) Reichardt, C. *Solvents and Solvent Effects in Organic Chemistry*; VCH: Weinheim, 1990.

(43) Wada, A. *J. Chem. Phys.* **1954**, *22*, 198.

(44) Wiberg, K. B.; Keith, T. A.; Frisch, M. J.; Murcko, M. *J. Phys. Chem.* **1995**, *99*, 9072.

(45) Wong, M. W.; Frisch, M. J.; Wiberg, K. B. *J. Am. Chem. Soc.* **1991**, *113*, 4776.

(46) Jorgensen, W. L.; McDonald, N. A.; Selmi, M.; Rablen, P. R. *J. Am. Chem. Soc.* **1995**, *117*, 11809.

(47) Abraham, R. J.; Siverns, T. M. *Tetrahedron* **1972**, *28*, 3015.

(48) For recent reviews, see: (a) Gajewski, J. J. *Acc. Chem. Res.* **1997**, *30*, 219. (b) Ganem, B. *Angew. Chem., Int. Ed. Engl.* **1996**, *35*, 289.

(49) Vance, R. L.; Rondan, N. G.; Houk, K. N.; Jensen, F.; Borden, W. T.; Komornicki, A.; Wimmer, E. *J. Am. Chem. Soc.* **1988**, *110*, 2314.

(50) Carlson, H. A.; Jorgensen, W. L. *J. Am. Chem. Soc.* **1996**, *118*, 8475.

(51) Cramer, C. J.; Truhlar, D. G. *J. Am. Chem. Soc.* **1992**, *114*, 8794.

(52) Gao, J. *J. Am. Chem. Soc.* **1994**, *116*, 1563.

(53) Sehgal, A.; Shao, L.; Gao, J. *J. Am. Chem. Soc.* **1995**, *117*, 11337.

(54) Davidson, M. M.; Hillier, I. H. *J. Phys. Chem.* **1995**, *99*, 6748.

(55) Wong, M. W.; Wiberg, K. B.; Frisch, M. J. *J. Am. Chem. Soc.* **1992**, *114*, 1645.

(56) (a) Cramer, C. J.; Truhlar, D. G. *J. Comput.-Aided Mol. Design* **1992**, *6*, 629. (b) Cramer, C. J.; Truhlar, D. G. *J. Am. Chem. Soc.* **1993**, *115*, 8810.

(57) Gao, J.; Shao, L. *J. Phys. Chem.* **1994**, *98*, 13772.

(58) Cieplak, P.; Bash, P.; Singh, U. C.; Kollman, P. A. *J. Am. Chem. Soc.* **1987**, *109*, 6283.

(59) Colominas, C.; Luque, F. J.; Orozco, M. *J. Am. Chem. Soc.* **1996**, *118*, 6811.

(60) Beak, P.; Fry, F. S. *J. Am. Chem. Soc.* **1973**, *95*, 1700.

(61) Frank, J.; Katrizky, A. R. *J. Chem. Soc., Perkin Trans. 2* **1976**, 1428.

(62) Mason, S. F. *J. Chem. Soc.* **1958**, 674.

(63) Albert, A.; Phillips, J. N. *J. Chem. Soc.* **1956**, 1294.